Laser-Assisted Simultaneous Transfer and Patterning of Vertically Aligned Carbon Nanotube Arrays on Polymer Substrates for Flexible Devices

Jung Bin In,[†,§] Daeho Lee,[†,§] Francesco Fornasiero,[‡] Aleksandr Noy,[‡] and Costas P. Grigoropoulos[†,*]

[†]Department of Mechanical Engineering, University of California Berkeley, Berkeley, California 94720-1740, United States, and [‡]Physical and Life Sciences Directorate, Lawrence Livermore National Laboratory, Livermore, California 94550, United States. [§]These authors contributed equally to this publication.

ABSTRACT

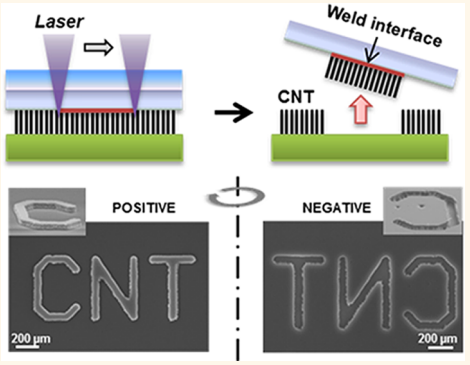

We demonstrate a laser-assisted dry transfer technique for assembling patterns of vertically aligned carbon nanotube arrays on a flexible polymeric substrate. A laser beam is applied to the interface of a nanotube array and a polycarbonate sheet in contact with one another. The absorbed laser heat promotes nanotube adhesion to the polymer in the irradiated regions and enables selective pattern transfer. A combination of the thermal transfer mechanism with rapid direct writing capability of focused laser beam irradiation allows us to achieve simultaneous material transfer and direct micropatterning in a single processing step. Furthermore, we demonstrate that malleability of the nanotube arrays transferred onto a flexible substrate enables post-transfer tailoring of electric conductance by collapsing the aligned nanotubes in different directions. This work suggests that the laser-assisted transfer technique provides an efficient route to using vertically aligned nanotubes as conductive elements in flexible device applications.

KEYWORDS: carbon nanotube · nanotube transfer · laser patterning · polymer substrate · flexible electronics

Carbon nanotubes (CNTs) have superior electric properties for various electronic applications including supercapacitors,[1] field effect transistors,[2] transparent electrodes,[3] and field emission displays.[4] Their significant mechanical elasticity also suggests potential uses in flexible devices based on polymeric substrates.[3,5−9] Vertically aligned carbon nanotubes (VACNTs), which grow *via* a self-assembling mechanism, offer a high degree of directionality that is highly desirable for controllable arrangement of this significantly anisotropic material on flexible substrates. Unfortunately, most polymeric flexible substrates are incompatible with the high temperature required for CNT growth. In order to incorporate synthesis of VACNTs into conventional device fabrication processes, researchers have developed various growth techniques to grow nanotubes at lower temperatures, mostly using a chemical vapor deposition (CVD) method.[10] Nonetheless, most CVD methods still require growth temperatures that are too high for the polymeric substrates. Thus, postgrowth CNT transfer provides a key opportunity to integrate this fascinating material with polymeric substrates and into flexible device architectures.

Various transfer techniques have been proposed to transfer as-grown VACNTs onto popular polymers such as polymethyl methacrylate (PMMA), polydimethylsiloxane (PDMS), polyethylene terephthalate (PET), and polycarbonate (PC).[5,11−13] Solution-based transfer is well-established and versatile (basically compatible with most substrates), but it is more adequate for deposition of a random network of nanotubes since VACNTs lose alignment in the dispersion process necessary for solubilization, and the subsequent evaporation of the solvent induces undesirable shrinkage of nanotubes.[11,14] In contrast, dry transfer methods maintain alignment of VACNTs as grown vertically or as collapsed horizontally by postgrowth rolling.[11,15,16] In principle, most dry transfer techniques are based on differential adhesion; for example, the CNT−(polymer receiver) interface has greater adhesion than the CNT−(growth substrate

* Address correspondence to cgrigoro@me.berkeley.edu.

Received for review May 17, 2012 and accepted August 10, 2012.

Published online August 11, 2012
10.1021/nn302192y

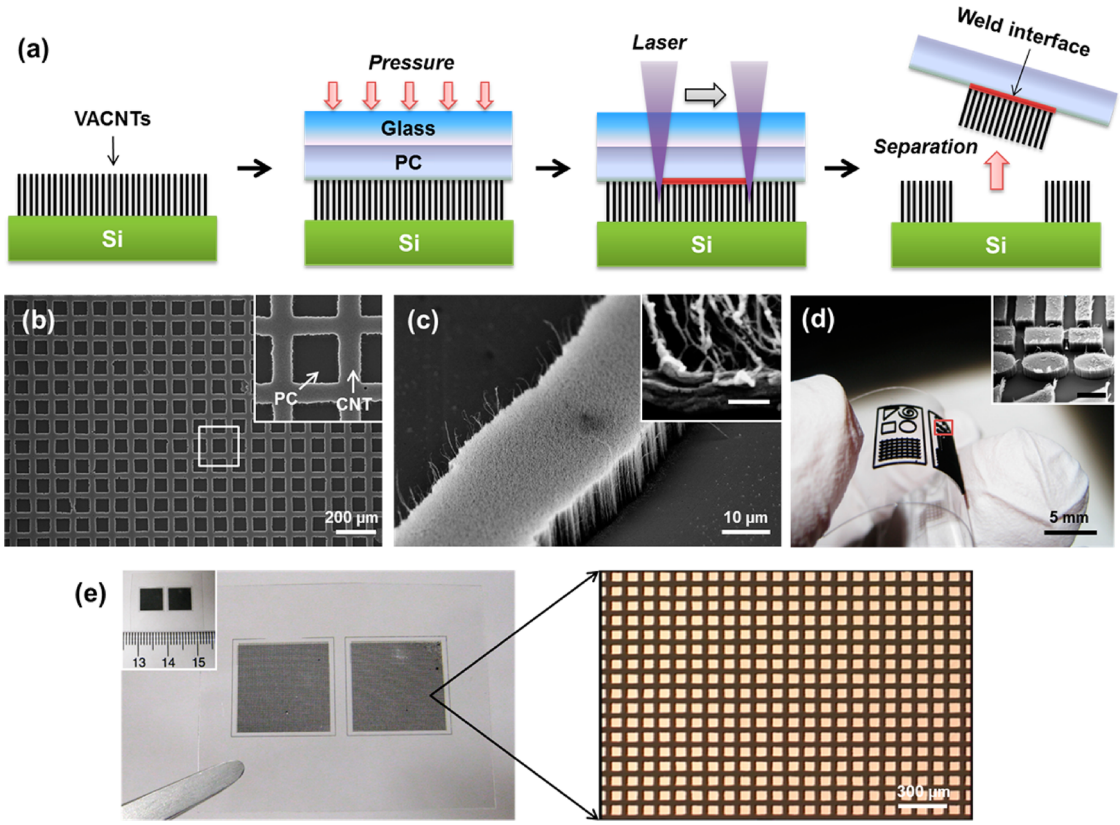

Figure 1. (a) Illustration of the laser-assisted VACNT transfer process. (b) SEM image (top view) of grid-patterned VACNTs on PC (125 μm thickness). The inset is an enlarged view of the marked area. A gold layer was coated on the sample to improve conductance for SEM imaging. (c) SEM image (oblique view) of transferred VACNTs on PC. The inset shows a high-magnification SEM image on the cross section near the VACNT–PC weld interface after tearing the polymer film (scale bar: 400 nm). Likewise, a gold layer was coated on the sample. (d) Photo image of the transferred VACNTs on a large scale. The inset shows the SEM image of the areal patterns in the marked area (scale bar: 400 μm). (e) Photo image (left) of a large-scale VACNT pattern and the corresponding optical microscope image (right) at the indicated position. The inset (left) shows the scale of the pattern (unit: cm).

donor) interface. Coating an additional adhesive layer on the target surface can promote transfer,[17] or sometimes even a van der Waals interaction is strong enough to detach the VACNTs and sustain the adherence to the receiver material, depending on the surface characteristic of the receiver.[11,16] In addition, adhesion induced by polymerization[18] or by heat[12,13,19] enables successful transfer of VACNTs to polymer receivers. Notably, previous studies focused on the transfer step; therefore, to fabricate VACNT patterns on the receiver substrate VACNTs were synthesized on a patterned catalyst area prior to the transfer, hence requiring additional metal patterning process steps.

In this paper, we propose a laser-assisted rapid dry transfer technique for VACNTs where laser-based direct writing is combined with the thermally induced dry transfer process. This combination allows simultaneous VACNT transfer onto flexible polymers as well as rapid micropatterning under ambient conditions, remarkably accelerating the overall patterning and transfer process. We also demonstrate the engineered alignment of the transferred VACNT forest and the tunability of its electrical conductance by applying a pressurized mechanical rolling process. Finally, we discuss the superior bendability of the transferred nanotubes based on measured electrical resistances under various bending conditions.

RESULT AND DISCUSSION

Laser-Assisted Transfer and Patterning. In our transfer procedure (Figure 1a) a general-purpose-grade PC sheet (McMaster-Carr) is placed on VACNTs grown by CVD on a silicon substrate, with the target surface of the PC facing the top of the VACNT forest. In addition, a glass slide imposes contact and flatness on the PC–VACNT interface over a laser scanning area (as illustrated in Figure S2). A simple mechanical clamping with spacers of a proper thickness is applied to pressurize the PC film toward the nanotubes. The mechanical pressure is maintained until the end of the laser scanning. The piled glass–PC–VACNT assembly is either translated under laser irradiation through the fixed objective lens or is held stationary while the galvanometer mirror system writes pattern lines (see Methods for the details of the laser system). The absorbed thermal energy from the laser beam fluidizes

the PC just adjacent to the interface, and the liquid or partially viscous polymer promptly wets the tips of nanotubes by capillary force.[12,20] As the laser beam passes, highly thermally conductive VACNTs rapidly dissipate the absorbed heat, completing the *laser welding* process. Afterward, due to the higher adhesion at the weld interface, the transplanted VACNTs are selectively peeled off the nanotube forest by exerting moderate separation force. All transfer steps are conducted under ambient conditions.

VACNTs were successfully transferred on the PC substrates (of 125 μm thickness) both by the UV laser setup (wavelength: 355 nm) with a 39× objective lens and by the argon laser (wavelength: 514 nm) with a galvanometer mirror system. The SEM images in Figure 1b, c show the morphologies of the transferred VACNTs by the UV laser setup. The inset in Figure 1c shows the transferred nanotubes whose ends are embedded in the PC. The smallest line width that we could reliably write was about 30 μm at a laser power of 15−20 mW and a scanning speed of 5 mm/s. Likewise, the argon laser beam directed by the X−Y galvanometer mirror system was effective in transferring nanotube patterns. The line width became larger (generally 50−75 μm) relative to the patterns produced with the UV laser at the corresponding laser power because of the enlarged focal spot size (50 μm). However, the galvanometer mirror system enabled high-speed patterning on a relatively large scale, highlighting practical aspects of the transfer method. For instance, the maximum scanning speed that allowed writing of a line pattern of VACNTs was approximately 1 m/s at an increased irradiation power of 220 mW. Figure 1d shows the various symbols of the transferred VACNTs that were marked by this scanning system. In contrast to the line patterns of Figure 1b, areal patterning (inset of Figure 1d) was produced using a serpentine scanning path that covered the inner area of the symbols. Scan overlapping guaranteed complete transfer. Figure 1e shows a centimeter-scale VACNT micropattern (1.8 cm × 0.9 cm) on a PC substrate, whose spatial uniformity demonstrates potential use of this laser-assisted transfer method in large-scale fabrication.

Transfer Mechanism. We note that the pressure exerted by the upper glass slide improves the contact between the PC film and the VACNTs, which is critical for successful transfer. Although the laterally interwoven structure of the top surface gives the as-grown VACNT forest good height uniformity,[21,22] some variation remains, especially on a relatively large scanning area. This is a typical issue in CVD growth that results from inhomogeneity in the CVD environment. Moreover, commercial PC films are prone to contain a structural curvature that is possibly generated by deformation during the material fabrication and handling. Without exerting additional force, an air gap

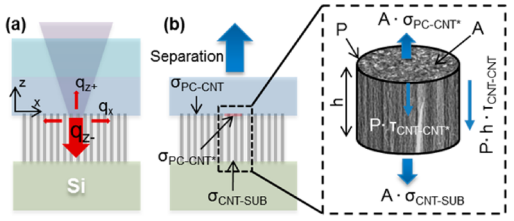

Figure 2. (a) Illustration of heat transfer during laser irradiation. (b) Mechanical model for the relation of static forces during the separation process (A: area of transfer pattern, P: perimeter of the pattern, h: height of nanotube forest).

would form between the PC surface and the top of the VACNT forest, leading to loss of local contact. In addition, the glass slide acts as a flat template that is required when high-magnification far-field illumination is applied to a translating target. Indeed, a facile transfer experiment without the pressurizing glass slide revealed that nanotubes were only partially transferred into broken patterns where the contact was lost or the laser beam focus deviated from the desired depth. Figure S3a shows a top view of the PC film where the transfer succeeded on the left side, whereas the transfer failed on the right side, only leaving evidence of thermal damage.

Even though the flattening glass compensates for height variation of VACNTs to a degree, the height uniformity of as-grown VACNTs is still crucial to avoid the possibility of severe deformation by compression. As the VACNTs are compressed, structural buckling may occur by excessive flattening force, resulting in significant waviness on the lateral morphology of the nanotubes. For instance, Cao *et al.*[23] reported that axial compressive strain over ∼22% induced collective and periodic buckling with a wavelength of ∼12 μm in the VACNTs. In our case, such structural damage will become inevitable if the height variance of VACNTs is too large to be elastically restored after relaxation of the compression. However, our experiment reveals that the transferred VACNTs do not experience noticeable buckling (Figure S4). Therefore, we believe that the height uniformity of the nanotube forest is key to mitigating the impact of buckling on the transfer process.

The temperature at the PC−VACNT interface is another key parameter for successful transfer since the PC film is thermally frail, with glass transition and melting temperatures of ∼150 and ∼230 °C, respectively.[24] For instance, excessive laser power damaged PC films severely, leaving a white residue without accomplishing any nanotube transfer. Interestingly, when a moderately high level of laser power was applied, nanotube transfer succeeded only on the tail area of the Gaussian energy profile to write double lines (Figure S3b). Figure 2a depicts the heat flow paths during laser irradiation for the nanotube transfer. VACNTs have much higher optical absorptivity than PC, with respect to the laser

wavelengths (λ = 355, 514 nm).[25,26] (In general, PC is known as a UV blocking polymer, but we measured ~90% transmittance when the UV laser (355 nm) was applied to the tested PC film of 125 μm thickness.) Notwithstanding the scattered reported values of thermal conductivity of VACNTs, VACNTs have orders of magnitude higher thermal conductivity ($k_{CNT,z}$: 1−250 W/m·K)[27,28] than PC (k_{PC}: ~0.2 W/m·K); accordingly, most of the absorbed heat flows down through the nanotubes to the silicon substrate that serves as a heat sink ($q_{z-} \gg q_{z+}$, q_x). Thus, the thermal resistances between the PC and the silicon affect the proper range of laser power for successful nanotube transfer. In our sample, we deposited an oxide layer as a diffusion barrier to promote activity of the catalysts during the CNT growth, and this layer also poses a thermal resistance. Indeed, we observed that laser power needed to be decreased to avoid excessive heating when we used longer nanotubes or a thicker oxide film.

While the laser power is easily adjustable, the far-field laser illumination can render the temperature of the CNT−PC interface very sensitive to the laser beam focal position. One may expect that the interface should be placed ideally at the focal plane. However, we intentionally defocused the laser spot by a few micrometers down into the nanotubes for several practical reasons. First, in addition to the nonuniformity in VACNT heights and possibly in PC thickness, it is challenging to maintain the interface level within a reasonable focal range, especially when high magnification is necessary to obtain a smaller beam spot on a relatively large scanning area. Second, carbon nanotubes have greater thermal tolerance compared to polymers, allowing a wider parametric window. It is well-known from thermo-gravimetric analysis that nanotubes can endure up to ~550 °C even under ambient air conditions.[29] In contrast, when the laser beam is focused inside the polymer, the polymer temperature can vary significantly with the scanning speed, due to the low thermal diffusivity of PC. For instance, when the scanning speed is transiently decelerated (or accelerated) at the serpentine pattern turns, the polymer temperature at the focal spot can deviate significantly from the proper temperature level. Third, anisotropic thermal properties of VACNTs are favorable since axial conduction prevails over the lateral heat diffusion that would cause widening of the pattern line.

The separation process is simple but requires balancing between the adhesion strengths (N/m^2) of laser-welded PC−CNT (σ_{PC-CNT^*}), CNT−substrate ($\sigma_{CNT\text{-}SUB}$), van der Waals PC−CNT (σ_{PC-CNT}), and the shear friction induced by the characteristic structure of VACNTs that are bundled and laterally interconnected.[30] Due to the extraordinarily strong interaction of the interwoven nanotubes at the top of VACNTs,[22,30,31] we consider two shear stress parameters: $\tau_{CNT\text{-}CNT}$ (N/m^2) on the side wall and $\tau_{CNT\text{-}CNT^*}$ (N/m) at the top pattern perimeter.

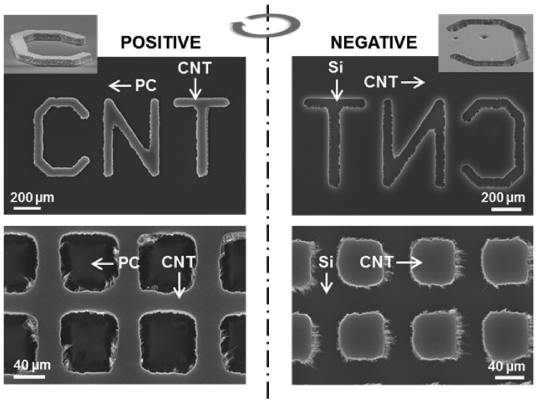

Figure 3. SEM images of dual patterns of VACNTs on the PC target substrate (left) and Si nanotube substrate (right), reminiscent of *decalcomania*. Each pattern has a mirror image with a reversed lithographic sign.

Here we model the top interwoven nanotube mat surface as a very thin two-dimensional network. First of all, $\sigma_{CNT-SUB}$ should be larger than σ_{PC-CNT} so that the area unaffected by laser does not transfer nanotubes. In this respect, the water etching, which reduces $\sigma_{CNT-SUB}$, prior to transfer[11,15] offers no advantage to our process. In addition, if we simplify the geometry of transfer pattern as described in Figure 2b, we obtain the following relation for successful transfer.

$$\sigma_{PC\ -\ CNT^*} > \sigma_{CNT\ -\ SUB} + \frac{P}{A}\left(h\tau_{CNT\ -\ CNT} + \tau_{CNT\ -\ CNT^*}\right) \quad (1)$$

where P is the perimeter of the pattern, A is the area of the pattern, and h is the height of the VACNTs. In the case of a cylindrical shape of transferring nanotubes, the geometry term (P/A) reduces to $2/R$. Despite the simplification followed in this derivation, eq 1 suggests important information on the separation process. Given the adhesion strengths of σ_{PC-CNT^*} and $\sigma_{CNT-SUB}$, the shear friction comes into play when the thickness of the VACNTs (h) is high or the shape of the pattern has a high perimeter to area ratio (P/A). Reversely, the effect of the shear force decreases by using short VACNTs with a pattern shape that has a low P/A ratio or by amplifying the adhesion forces (σ_{PC-CNT^*}, $\sigma_{CNT-SUB}$). In this case, the adhesion relation for successful transfer will reduce to a simpler form:

$$\sigma_{PC\ -\ CNT^*} > \sigma_{CNT\ -\ SUB} > \sigma_{PC\ -\ CNT} \quad (2)$$

Although our transfer experiment does not render quantitative values for the adhesion forces and those values should also be dependent on the growth conditions of the VACNTs, our results still provide substantial evidence supporting this model. We observed that just pressing a PC sheet down to the nanotube forest did not allow transfer of the nanotubes. The PC surface of the nonpatterned area was free of nanotubes, which clearly satisfies the condition of $\sigma_{CNT-SUB} > \sigma_{PC-CNT}$. Interestingly, the separation process generated

suspended strands of nanotubes that were pulled out by shear force but still remained attached to the side wall of VACNTs (Figure 1c) (also see Figure S5 in the Supporting Information). Moreover, the shear force resulted in transfer of extra nanotube material near acute corners of pattern lines. Indeed, the presence of suspended strands and the loss of sharpness at the corners of the patterns were more pronounced with longer VACNTs, which can be confirmed by comparison of the inset of Figure 1b (10 μm thick) and Figure 3 (26 μm thick). As a positive side of this observation, however, we speculate that the shear force helps mitigate microscopic inhomogeneity in VACNT heights by pulling out the interlaced short nanotubes altogether. The suspended nanotube debris could be removed to a degree by contacting the surface of the pattern with a moderately tacky tape. The debris could also be pushed and attached to the side wall by capillary-driven shrinkage[11] at the expense of morphological reconfiguration of the VACNTs (Figure S6).

Our transfer method shares the basic mechanism and technical advantages with the thermal method proposed by Tsai *et al.*,[12] but the laser transfer is distinguished by several features. Above all, it achieves maskless direct writing simultaneously with the location-controlled material transfer, providing a very versatile one-step process for VACNT patterning on polymeric substrates. Furthermore, laser illumination confines the heat-affected area and thereby minimizes the thermal damage so that VACNTs can be transferred onto thinner polymer films. This advantage was more noticeable when thermal transfer was conducted on a hot plate at 155 °C by heating the entire polymer film. These experiments showed that the thinner PC film (125 μm) is more vulnerable to heat damage, resulting in irreversible deformation, whereas the thicker (500 μm) film allowed nanotube transfer with reasonably small deformation, as demonstrated by Tsai *et al.* In contrast, laser-assisted transfer enabled successful transfer of VACNTs to both films.

Additionally, the laser transfer produces dual patterns with pairs of mirror images, as shown in Figure 3, one on the PC and the other on the silicon, in a process reminiscent of *decalcomania*. This secondary or remnant nanotube pattern on the silicon side indicates that the corresponding technique can be applied not only for patterning on polymer films but also for VACNT patterning on the Si substrate. Instead, the lithographic sign gets reversed; on the polymer side, the transferred VACNTs stay on the scanned area (positive), while on the silicon substrate side, the irradiated nanotubes are subtracted from the VACNT forest (negative).

Despite the aforementioned advantages of the laser-assisted transfer, this method has its limitation on the selection of substrate materials. While melting temperatures of most polymers belong to a proper range for this technique, adhesion between nanotubes and specific polymers can fail to satisfy conditions for successful transfer (eq 2). In order to explore material compatibility, we have examined additional kinds of polymers: PET, PMMA, PDMS, and polyimide (PI). We used the green laser (wavelength: 514 nm) to write line patterns on them. We found that PET and PMMA were successful for the transfer, but PDMS tended to transfer even nonscanned nanotubes, possibly due to the intrinsic tackiness of the PDMS surface (in other words, relatively large $\sigma_{PDMS-CNT}$). PI is not as optically transparent as the other polymers, and it did not allow the laser transfer. When we used a hot plate (415 °C) to confirm the transfer compatibility, nanotubes could be transferred to PI. However, the adhesion was poor (relatively small σ_{PI-CNT^*}) and the transferred nanotubes could be easily detached by other tacky surfaces such as PDMS.

Tailoring of Electrical Resistance. Notwithstanding the phenomenal electrical transport properties of individual CNTs, VACNTs have in practice several orders of magnitude lower conductivity than theoretical predictions, due to structural defects on the nanotube walls and incomplete contact to electrodes.[16] Furthermore, the anisotropic nature of VACNT arrays limits their lateral conductivity by at least an order of magnitude lower than that in the axial direction.[32] In our case, the measured conductivity of as-transferred VACNTs (or V-CNT) was about 0.4−0.6 ($\Omega^{-1}\cdot cm^{-1}$) in the lateral (*x*-axis) direction. (Here we designate the transferred VACNTs on PC as V-CNT.) In this regard, various efforts have been made to improve electrical conduction of VACNTs; the most promising one is densification of VACNTs by capillary-driven shrinkage,[14] mechanical compression using a rigid roller,[11] or a combination of both.[16]

In this study, we adopted the mechanical roller method to enhance the conductance of the transferred VACNTs. More importantly, we also examined the post-transfer tunability of the resistance by collapsing the VACNTs in different directions, based on the highly anisotropic conductivity of VACNTs. Multiple laser transfers were conducted to prepare a single strip of V-CNT (75 μm × 70 μm × 3.5 mm, W × H × L) on PC substrates. After measurement of the intrinsic conductance (G_V), each V-CNT line was directionally compressed by collapsing the vertical nanotubes with a mechanical roller in different directions, *i.e.* the longitudinal (H-CNT), perpendicular (P-CNT), and diagonal (D-CNT) directions, as illustrated in Figure 4a. In accordance with the previous reports,[5,14,16,33] an ohmic *I*−*V* relation with increased conductance (d*I*/d*V*, Ω^{-1}) was obtained due to the enhanced connectivity between neighboring CNTs by the applied packing.

Interestingly, not only did the conductance increase, but directional enhancement was also obtained in the order of H-, D-, P-, and V-CNT, as shown in Figure 4b. For more quantitative comparison, we

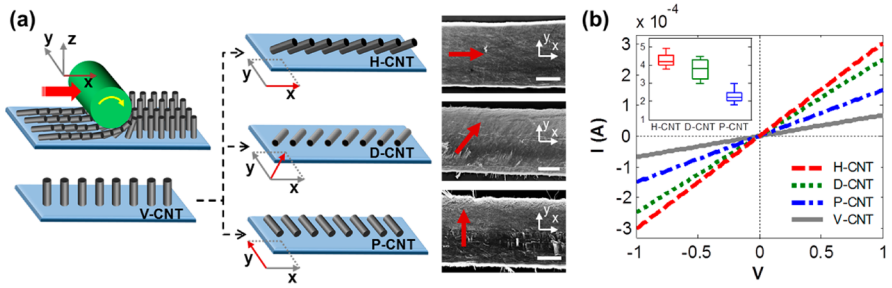

Figure 4. (a) Illustration of directional collapse by the mechanical rolling process. The SEM images (top view) show the directional morphologies of the roller-pressed nanotubes on PC substrates (scale bar: 40 μm). The red arrows indicate the corresponding directions of rolling. (b) Representative $I-V$ curves of transferred VACNT filaments after the roller process. The inset indicates the calculated conductance enhancement factors (G_H/G_V, G_D/G_V, G_P/G_V) out of multiple collapsed nanotube lines.

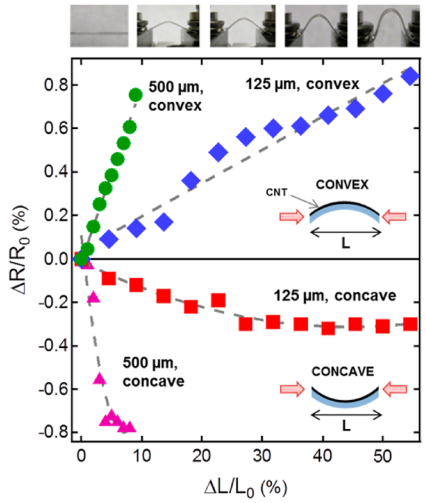

Figure 5. Normalized resistance change (%) of the transferred nanotubes on PC sheets (125, 500 μm thick) by bending. The convex or concave mode indicates the shape of the transferred nanotube surface. The data fits of the convex mode are linear, and the fits of the concave mode are parabolic. The photo images show a series of deformation by the convex bending.

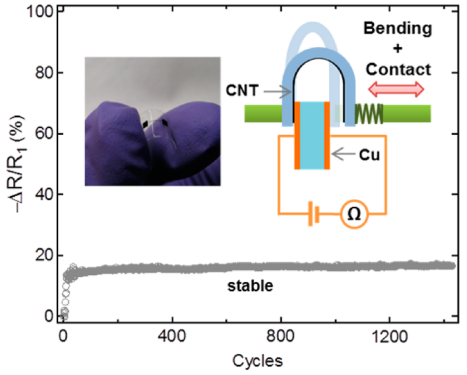

Figure 6. Normalized resistance change (%) in the cyclic reliability test. R_1 indicates the resistance of the first cycle. The photo inset (left) shows the examined pad and line element of transferred VACNTs on a PC sheet (125 μm thick). The bending radius cycles between 0.63 and 0.79 mm for repeated on and off of the open circuit that the inset schematic (right) depicts.

define the conductance enhancement factor as the ratio of the conductance of the tailored nanotubes to the prior (intrinsic) value of V-CNT, for example, G_H/G_V for H-CNT. The enhancement factor of H-CNT was highest up to 5-fold (inset of Figure 4b). As the lengths of the individual nanotubes are much shorter than the length of the whole V-CNT strip, electron transport *via* internanotube channel is inevitable. Accordingly, we ascribe this directional enhancement to the vectorial contribution of rapid one-dimensional conduction of nanotubes along the strip direction (*x*-axis). We believe that this postgrowth and post-transfer tailoring of nanotube conductance paves a new way to adjust the conductance of aligned nanotubes.

Bendability Tests. There have been various studies on piezoresistive behavior of carbon nanotubes in the form of transferred film[6,12,34] or composite with polymers.[5,35,36] This property is related to the change in the collective resistance of nanotubes by mechanical strain. We also examined this behavior with our transferred VACNTs (V-CNT). To investigate the resistance change of a strip of the VACNTs (on 125 and 500 μm thick PC substrates), we imposed gradually increasing mechanical bending as the schematics and the photos in Figure 5 depict. The bending parameter is determined as a ratio of the distance change (ΔL) to the original length (L_0). The measured resistance variation (%) is also shown in Figure 5. The convex or concave mode indicates the shape of the bent PC sheet while the surface of the transferred nanotubes faces upward.

The resistance variation can be understood in the context of the aforementioned relation of conductance and density of VACNTs. In the convex mode, the strain along the nanotube−PC interface works in a stretching fashion, resulting in a reduced density. In contrast, the concave mode induces packing of the nanotubes. Hence, the resistance increases with bending in the convex mode, whereas the opposite trend is the case in the concave mode. It is noted that the resistance of the concave bending decreases as the bending curvature increases but converges asymptotically to a plateau, indicating that the resistance

reduction mechanism saturates earlier than its counterpart. Although the obtained data with the 125 μm thick PC sheet are qualitatively consistent with the result of Tsai *et al.*,[12] the degree of bending ($\Delta L/L_0$) is about 12-fold extended under the same level of resistance change. As seen in Figure 5, however, the resistance variation of the VACNT array becomes more sensitive to the bending parameter with the thicker (500 μm) PC sheet. The data prove that the tolerance to bending originates from nothing other than the reduced level of strain at the surface of the thinner PC. On the basis of the above argument, we suggest that nanotubes on thinner PC sheets are more preferred for the application of flexible devices, while nanotubes on thicker sheets have an advantage as a possible strain gauge.

In order to investigate the electrical contact[37] and bending endurance[35] simultaneously, a simple yet efficient characterization method was designed (insets of Figure 6). A VACNT (70 μm thick) interconnect consisting of a line element and VACNT pads (1.5 $\times$ 1.5 mm^2) at each end was transferred on a PC substrate (125 μm thick). One of the pads was fixed for contact to the one Cu electrode of the circuit, whereas the other pad was attached to a motorized linear stage to engage or disengage the pad to the other electrode for on-and-off of the circuit. As the stage travels, the VACNT line array was also subject to continuous bending approximately from the bending radius 0.79 mm (off) to 0.63 mm (on). Finally, a cyclic test was conducted by moving the stage back and forth, repeatedly. The plot in Figure 6 indicates the recorded resistance during over 1400 cycles in ambient conditions. Due to the extreme degree of bending,[35] the nanotubes underwent an irreversible change in the resistance up to 14% during the first 10 cycles. After the test, we observed that even the PC sheet was under significant plastic deformation. However, the resistance stabilized soon with no significant change in the value. We attribute this superior bendability and reliable contact to the strong adhesion of the nanotubes to the PC sheet by our laser method and also to the mechanical compliance of nanotubes with external force.[37]

Our tests demonstrate that the laser-transferred nanotubes on PC sheets could be promising materials for layer-crossing and foldable interconnects[16,18] or switches for flexible devices, which represents a valuable integration of nanomaterials and polymers. We also suggest that when applied to transfer of semiconducting single-walled carbon nanotubes, this technique can be used for fabrication of flexible field effect transistor devices.[13] Lastly, we note that our straightforward approach enables cheap VACNT device fabrication not only as a direct writing process but also as an area-selective and material-saving process. For instance, the laser-assisted transfer consumes a local nanotube area on a large-scale VACNT forest, and the remaining nontransferred VACNTs on the donor substrate can be successively reused for subsequent transfer processes.

CONCLUSIONS

In conclusion, we have developed a versatile laser-assisted dry transfer technique for rapid pattering of VACNTs on polymeric substrates. Our work provides a direct and fast route to patterning of VACNTs on PC sheets with no need for conventional photolithographic processes that are normally used for CVD growth catalyst patterning. We believe the proposed method is also scalable to a larger size, while the maximum pattern and transfer size we obtained was about 2 $\times$ 2 cm^2 due to the dimensional limit of the nanotube growth system. Still, tight control on height uniformity of VACNTs is necessary to pursue our transfer technique on a wafer scale. Laser-induced strong adhesion of nanotubes to PC sheets allows the transferred nanotubes to be mechanically engineered to produce adjustable conductance. Localized heating by laser also minimizes thermal deformation and thereby enables VACNT transfer onto thinner PC sheets. Transferred VACNTs on thin flexible PC substrates demonstrate extreme bendability with great repeatability. We therefore suggest that not only is the laser-assisted method advantageous for nanotube transfer but also the resulting integration of VACNTs with polymers could be used to manufacture reliable conductive interconnects for flexible devices.

METHODS

CVD Synthesis of VACNTs. VACNTs that consist of single- and multiwalled nanotubes (2−5 nm diameter) were synthesized at 750 °C by atmospheric pressure chemical vapor deposition. Thin catalyst films of iron (2 nm)/alumina (30 nm) were deposited on a silicon(100) substrate by e-beam evaporation and sputtering, respectively. Catalyst patterning was not necessary, but growth conditions were fine-tuned to obtain a uniform VACNT forest. The detailed nanotube growth procedure was described in our previous work.[38]

Laser Irradiation Setup. In order to examine the feasibility of the proposed method on various scales, we use two different vertical laser illumination setups that have different optical specifications. In the first system, an as-grown nanotube chip is located on the motorized X−Y stage that is coupled with a vertical laser illumination setup: yttrium vanadate (Nd:YVO4) picosecond laser (Spectra-Physics, wavelength: 355 nm, pulse width (fwhm): 12 ps, repetition rate: 80 MHz) *via* a 39$\times$ objective (NA = 0.5) lens. This setup is used to transfer nanotube patterns of smaller features. The second setup adopts a galvanometer mirror system (SCANLAB hurrySCAN II-14) coupled with an argon laser (Lexel 3000, λ = 514 nm, continuous wave). Galvanometer mirror systems are widely used for high-speed laser marking by controllably reflecting the incoming laser beam

onto a two-dimensional target plane, instead of moving the target material. Accordingly, they avoid inertial load of motorized stages, and, thereby, this enables highly dynamic and rapid scanning with minimal spatial requirement. In this case, the nanotube chip stays fixed during laser irradiation. (The system schematics are also shown in Figure S1.)

Measurement of Electric Resistance. A rigid roller (0.5 cm diameter glass rod) was used with a moderate force to collapse the transferred VACNTs to a desired direction. A sheet of aluminum foil was mediated between VACNTs and the rod to prevent the CNT from sticking to the rod.[11] After the rolling process, a constant force (85 N) was applied to further densify the collapsed nanotubes. The resistance was measured using a two-probe technique with a HP 4155A semiconductor parameter analyzer at room temperature. To reduce the contact resistance between the VACNTs and probe tips, silver paste was applied at each end of the nanotube line.

Bendability Test. For the bendability test, one end of the VACNTs transferred to a PC substrate was attached to a motorized stage, while the other end was fixed. The resistance was measured as the stage moved by an equal distance, increasing the bending curvature gradually. Especially for the bendability test in Figure 5, gallium−indium eutectic alloy (Sigma-Aldrich) was applied to the contact interface of the VACNT line array and the probe electrode to maintain more reliable and robust electric contact against the deformation of the PC sheet. For the bending+contact test (Figure 6), the reverse side of the VACNTs pads was attached respectively to the fixed wall and to the coil spring (k_s ~4.1 N/mm) that was attached to a motorized linear stage. The moving pad was compressed until the obtained resistance reduced to a stable level. As the stage traveled repeatedly back and forth, the VACNTs were subject to continuous bending while the pads underwent repetitive contacts to the copper electrodes. The resistance data were logged in a computer system.

Conflict of Interest: The authors declare no competing financial interest.

Acknowledgment. This work was supported by the SINAM NSF NSEC. The authors also thank the King Abdullah University of Science and Technology (KAUST) for the support through a grant to the ME Dept. of UC Berkeley. J.I. thanks Dr. Hojeong Jeon for assistance with microscope imaging.

Supporting Information Available: Additional data and figures as described in the text. This material is available free of charge *via* the Internet at http://pubs.acs.org.

REFERENCES AND NOTES

1. Simon, P.; Gogotsi, Y. Materials for Electrochemical Capacitors. *Nat. Mater.* **2008**, *7*, 845–854.
2. Artyukhin, A. B.; Stadermann, M.; Friddle, R. W.; Stroeve, P.; Bakajin, O.; Noy, A. Controlled Electrostatic Gating of Carbon Nanotube FET Devices. *Nano Lett.* **2006**, *6*, 2080–2085.
3. Wu, Z. C.; Chen, Z. H.; Du, X.; Logan, J. M.; Sippel, J.; Nikolou, M.; Kamaras, K.; Reynolds, J. R.; Tanner, D. B.; Hebard, A. F.; *et al*. Transparent, Conductive Carbon Nanotube Films. *Science* **2004**, *305*, 1273–1276.
4. Fan, S. S.; Chapline, M. G.; Franklin, N. R.; Tombler, T. W.; Cassell, A. M.; Dai, H. J. Self-Oriented Regular Arrays of Carbon Nanotubes and Their Field Emission Properties. *Science* **1999**, *283*, 512–514.
5. Jung, Y. J.; Kar, S.; Talapatra, S.; Soldano, C.; Viswanathan, G.; Li, X. S.; Yao, Z. L.; Ou, F. S.; Avadhanula, A.; Vajtai, R.; *et al*. Aligned Carbon Nanotube-Polymer Hybrid Architectures for Diverse Flexible Electronic Applications. *Nano Lett.* **2006**, *6*, 413–418.
6. Yamada, T.; Hayamizu, Y.; Yamamoto, Y.; Yomogida, Y.; Izadi-Najafabadi, A.; Futaba, D. N.; Hata, K. A Stretchable Carbon Nanotube Strain Sensor for Human-Motion Detection. *Nat. Nanotechnol.* **2011**, *6*, 296–301.
7. Sekitani, T.; Noguchi, Y.; Hata, K.; Fukushima, T.; Aida, T.; Someya, T. A Rubberlike Stretchable Active Matrix Using Elastic Conductors. *Science* **2008**, *321*, 1468–1472.
8. Hu, C. F.; Su, W. S.; Fang, W. L. Development of Patterned Carbon Nanotubes on a 3d Polymer Substrate for the Flexible Tactile Sensor Application. *J. Micromech. Microeng.* **2011**, *21*, 115012.
9. Lee, D. H.; Lee, J. A.; Lee, W. J.; Kim, S. O. Flexible Field Emission of Nitrogen-Doped Carbon Nanotubes/Reduced Graphene Hybrid Films. *Small* **2011**, *7*, 95–100.
10. Cantoro, M.; Hofmann, S.; Pisana, S.; Scardaci, V.; Parvez, A.; Ducati, C.; Ferrari, A. C.; Blackburn, A. M.; Wang, K. Y.; Robertson, J. Catalytic Chemical Vapor Deposition of Single-Wall Carbon Nanotubes at Low Temperatures. *Nano Lett.* **2006**, *6*, 1107–1112.
11. Pint, C. L.; Xu, Y. Q.; Pasquali, M.; Hauge, R. H. Formation of Highly Dense Aligned Ribbons and Transparent Films of Single-Walled Carbon Nanotubes Directly from Carpets. *ACS Nano* **2008**, *2*, 1871–1878.
12. Tsai, T. Y.; Lee, C. Y.; Tai, N. H.; Tuan, W. H. Transfer of Patterned Vertically Aligned Carbon Nanotubes onto Plastic Substrates for Flexible Electronics and Field Emission Devices. *Appl. Phys. Lett.* **2009**, *95*, 013107.
13. Tseng, S. H.; Tai, N. H. Fabrication of a Transparent and Flexible Thin Film Transistor Based on Single-Walled Carbon Nanotubes Using the Direct Transfer Method. *Appl. Phys. Lett.* **2009**, *95*, 204104.
14. Futaba, D. N.; Hata, K.; Yamada, T.; Hiraoka, T.; Hayamizu, Y.; Kakudate, Y.; Tanaike, O.; Hatori, H.; Yumura, M.; Iijima, S. Shape-Engineerable and Highly Densely Packed Single-Walled Carbon Nanotubes and Their Application as Supercapacitor Electrodes. *Nat. Mater.* **2006**, *5*, 987–994.
15. Pint, C. L.; Xu, Y. Q.; Moghazy, S.; Cherukuri, T.; Alvarez, N. T.; Haroz, E. H.; Mahzooni, S.; Doorn, S. K.; Kono, J.; Pasquali, M.; *et al*. Dry Contact Transfer Printing of Aligned Carbon Nanotube Patterns and Characterization of Their Optical Properties for Diameter Distribution and Alignment. *ACS Nano* **2010**, *4*, 1131–1145.
16. Tawfick, S.; O'Brien, K.; Hart, A. J. Flexible High-Conductivity Carbon-Nanotube Interconnects Made by Rolling and Printing. *Small* **2009**, *5*, 2467–2473.
17. Qu, L. T.; Vaia, R. A.; Dai, L. M. Multilevel, Multicomponent Microarchitectures of Vertically-Aligned Carbon Nanotubes for Diverse Applications. *ACS Nano* **2011**, *5*, 994–1002.
18. Zhu, Y. W.; Lim, X. D.; Sim, M. C.; Lim, C. T.; Sow, C. H. Versatile Transfer of Aligned Carbon Nanotubes with Polydimethylsiloxane as the Intermediate. *Nanotechnology* **2008**, *19*, 325304.
19. Zhang, G. Y.; Mann, D.; Zhang, L.; Javey, A.; Li, Y. M.; Yenilmez, E.; Wang, Q.; McVittie, J. P.; Nishi, Y.; Gibbons, J.; *et al*. Ultra-High-Yield Growth of Vertical Single-Walled Carbon Nanotubes: Hidden Roles of Hydrogen and Oxygen. *Proc. Natl. Acad. Sci. U. S. A.* **2005**, *102*, 16141–16145.
20. Ding, W.; Eitan, A.; Fisher, F. T.; Chen, X.; Dikin, D. A.; Andrews, R.; Brinson, L. C.; Schadler, L. S.; Ruoff, R. S. Direct Observation of Polymer Sheathing in Carbon Nanotube-Polycarbonate Composites. *Nano Lett.* **2003**, *3*, 1593–1597.
21. Zhang, Q.; Zhou, W. P.; Qian, W. Z.; Xiang, R.; Huang, J. Q.; Wang, D. Z.; Wei, F. Synchronous Growth of Vertically Aligned Carbon Nanotubes with Pristine Stress in the Heterogeneous Catalysis Process. *J. Phys. Chem. C* **2007**, *111*, 14638–14643.
22. Bedewy, M.; Meshot, E. R.; Guo, H. C.; Verploegen, E. A.; Lu, W.; Hart, A. J. Collective Mechanism for the Evolution and Self-Termination of Vertically Aligned Carbon Nanotube Growth. *J. Phys. Chem. C* **2009**, *113*, 20576–20582.
23. Cao, A. Y.; Dickrell, P. L.; Sawyer, W. G.; Ghasemi-Nejhad, M. N.; Ajayan, P. M. Super-Compressible Foamlike Carbon Nanotube Films. *Science* **2005**, *310*, 1307–1310.
24. Brandrup, J.; Immergut, E. H.; Grulke, E. A.; Abe, A.; Bloch, D. R. *Polymer Handbook*, 4th ed.; John Wiley & Sons: New York, 1999.
25. Mizuno, K.; Ishii, J.; Kishida, H.; Hayamizu, Y.; Yasuda, S.; Futaba, D. N.; Yumura, M.; Hata, K. A Black Body Absorber from Vertically Aligned Single-Walled Carbon Nanotubes. *Proc. Natl. Acad. Sci. U. S. A.* **2009**, *106*, 6044–6047.

26. Yang, Z. P.; Ci, L. J.; Bur, J. A.; Lin, S. Y.; Ajayan, P. M. Experimental Observation of an Extremely Dark Material Made by a Low-Density Nanotube Array. *Nano Lett.* **2008**, *8*, 446–451.
27. Ivanov, I.; Puretzky, A.; Eres, G.; Wang, H.; Pan, Z. W.; Cui, H. T.; Jin, R. Y.; Howe, J.; Geohegan, D. B. Fast and Highly Anisotropic Thermal Transport through Vertically Aligned Carbon Nanotube Arrays. *Appl. Phys. Lett.* **2006**, *89*, 223110.
28. Tong, T.; Zhao, Y.; Delzeit, L.; Kashani, A.; Meyyappan, M.; Majumdar, A. Dense, Vertically Aligned Multiwalled Carbon Nanotube Arrays as Thermal Interface Materials. *IEEE Trans. Compon., Packag. Technol.* **2007**, *30*, 92–100.
29. Hata, K.; Futaba, D. N.; Mizuno, K.; Namai, T.; Yumura, M.; Iijima, S. Water-Assisted Highly Efficient Synthesis of Impurity-Free Single-Waited Carbon Nanotubes. *Science* **2004**, *306*, 1362–1364.
30. Kuznetsov, A. A.; Fonseca, A. F.; Baughman, R. H.; Zakhidov, A. A. Structural Model for Dry-Drawing of Sheets and Yarns from Carbon Nanotube Forests. *ACS Nano* **2011**, *5*, 985–993.
31. Han, J. H.; Graff, R. A.; Welch, B.; Marsh, C. P.; Franks, R.; Strano, M. S. A Mechanochemical Model of Growth Termination in Vertical Carbon Nanotube Forests. *ACS Nano* **2008**, *2*, 53–60.
32. Lin, C. T.; Lee, C. Y.; Chin, T. S.; Xiang, R.; Ishikawa, K.; Shiomi, J.; Maruyama, S. Anisotropic Electrical Conduction of Vertically-Aligned Single-Walled Carbon Nanotube Films. *Carbon* **2011**, *49*, 1446–1452.
33. Bin, Z.; Futaba, D. N.; Yasuda, S.; Akoshima, M.; Yamada, T.; Hata, K. Exploring Advantages of Diverse Carbon Nanotube Forests with Tailored Structures Synthesized by Supergrowth from Engineered Catalysts. *ACS Nano* **2009**, *3*, 108–114.
34. Cohen, D. J.; Mitra, D.; Peterson, K.; Maharbiz, M. M. A Highly Elastic, Capacitive Strain Gauge Based on Percolating Nanotube Networks. *Nano Lett.* **2012**, *12*, 1821–1825.
35. Shin, M. K.; Oh, J.; Lima, M.; Kozlov, M. E.; Kim, S. J.; Baughman, R. H. Elastomeric Conductive Composites Based on Carbon Nanotube Forests. *Adv. Mater.* **2010**, *22*, 2663–2667.
36. Gui, X.; Li, H.; Zhang, L.; Jia, Y.; Liu, L.; Li, Z.; Wei, J.; Wang, K.; Zhu, H.; Tang, Z.; *et al*. A Facile Route to Isotropic Conductive Nanocomposites by Direct Polymer Infiltration of Carbon Nanotube Sponges. *ACS Nano* **2011**, *5*, 4276–4283.
37. Toth, G.; Maklin, J.; Halonen, N.; Palosaari, J.; Juuti, J.; Jantunen, H.; Kordas, K.; Sawyer, W. G.; Vajtai, R.; Ajayan, P. M. Carbon-Nanotube-Based Electrical Brush Contacts. *Adv. Mater.* **2009**, *21*, 2054–2058.
38. In, J. B.; Grigoropoulos, C. P.; Chernov, A. A.; Noy, A. Growth Kinetics of Vertically Aligned Carbon Nanotube Arrays in Clean Oxygen-Free Conditions. *ACS Nano* **2011**, *5*, 9602–9610.